

Large work extraction and the Landauer limit in a continuous Maxwell demon

M. Ribezzi-Crivellari^{1,2} and F. Ritort^{1,3*}

The relation between entropy and information dates back to the classical Maxwell demon paradox¹, a thought experiment proposed in 1867 by James Clerk Maxwell to violate the second law of thermodynamics. A variant of the classical Maxwell demon is the Szilard engine, proposed by Leo Szilard in 1929¹. In it, at a given time, the demon observes the compartment occupied by a single molecule in a vessel and extracts work by operating a pulley device. Here, we introduce the continuous Maxwell demon, a device capable of extracting arbitrarily large amounts of work per cycle by repeated measurements of the state of a system, and experimentally test it in single DNA hairpin pulling experiments. In the continuous Maxwell demon, the demon monitors the state of the DNA hairpin (folded or unfolded) by observing it at equally spaced time intervals, but it extracts work only when the molecule changes state. We demonstrate that the average maximum work per cycle that can be extracted by the continuous Maxwell demon is limited by the information content of the stored sequences, in agreement with the second law. Work extraction efficiency is found to be maximal in the large information-content limit where work extraction is fuelled by rare events.

In the Szilard engine, the demon performs a one-bit measurement by observing, at a given time, the compartment occupied by a single molecule in a vessel of volume V at temperature T (Fig. 1a). The engine operates as follows: if the molecule occupies the left compartment (V_0), a pulley device extracts the mean work $W_0 = -k_B T \log P_0$, where k_B is the Boltzmann constant and $P_0 = V_0/V$ is the probability of the molecule observed in the left compartment; if it occupies the right compartment ($V_1 = V - V_0$), the mean extracted work is $W_1 = -k_B T \log P_1$, with probability $P_1 = 1 - P_0$. The maximum average work per cycle that can be extracted in the classical Maxwell demon (MD) is

$$W_{\max}^{\text{MD}} = P_0 W_0 + P_1 W_1 = -k_B T (P_0 \log P_0 + P_1 \log P_1) \quad (1)$$

It is maximal for $P_0 = P_1 = 1/2$, $W_{\max}^{\text{MD}} \leq W_L = k_B T \log 2$, with W_L being the Landauer limit. The resolution of the MD paradox, that is, the fact that the engine can fully convert heat into work without any other change, came from the thermodynamics of data processing. Half a century ago, it was shown that any irreversible logical operation, such as bit erasure, requires energy consumption typically of the order of $k_B T$ (refs. 2,3). In general, W_{\max}^{MD} is equal to the information content I of one bit, $-P_0 \log P_0 - P_1 \log P_1$, restoring the second-law inequality

$$W \leq W_{\max}^{\text{MD}} = k_B T I \quad (2)$$

with W being the mean extracted work. Subsequent developments in experimental physics, often in combination with theorems of

fluctuation and information feedback^{4–8}, have provided experimental realizations and models of the MD that have tested equation (2) and the Landauer limit^{9–16}.

Here, we introduce the continuous MD (CMD), an information-to-energy conversion device that takes advantage of extracting work from rare events. The CMD is exemplified in Fig. 1b. The demon monitors the motion of the molecule by observing it at equally spaced time intervals τ , but extracts work only when the molecule changes compartment. A work extraction cycle starts with an initial observation of the compartment occupied by the molecule, which can be 0 (left compartment) or 1 (right compartment), followed by a series of repeated measurements every τ until the molecule changes compartment. We classify cycles into two classes, 0-cycles and 1-cycles, for cycles with an initial outcome measurement equal to 0 and 1, respectively. This is then followed by a series of $n-1$ repeated measurements of equal outcome made at times $\tau, 2\tau, 3\tau, \dots, (n-1)\tau$ until the molecule changes compartment at time $n\tau$: $0 \rightarrow 1$ for a 0-cycle and $1 \rightarrow 0$ for a 1-cycle. For cycles containing multiple observations, the demon stores in memory the $(n+1)$ -bit sequence containing n equal measurement outcomes plus the final (different) outcome. Stored sequences are defined as $0_n = \{0, \dots, 0, 1\}$ for 0-cycles and $1_n = \{1, \dots, 1, 0\}$ for 1-cycles ($n \geq 1$). The mean work per cycle depends on the last bit in the cycle and is $W_1 = -k_B T \log P_1$ for 0-cycles and $W_0 = -k_B T \log P_0$ for 1-cycles. The average maximum work per cycle that can be extracted by the CMD is independent of the time interval τ and is given by

$$W_{\max}^{\text{CMD}} = P_0 W_1 + P_1 W_0 = -k_B T (P_0 \log P_1 + P_1 \log P_0) \quad (3)$$

with P_0 and P_1 being the probabilities of 0-cycles and 1-cycles, respectively (that is, determined by the initial bit in the cycle). Albeit similar to equation (2), the functional dependence of W_{\max}^{CMD} on P_0 in equation (3) is different (Fig. 1c). In particular, W_{\max}^{CMD} in equation (3) is minimal (rather than maximal) for $P_0 = P_1 = 1/2$, the Landauer limit being a lower (rather than an upper) bound, $W_{\max}^{\text{CMD}} > W_L = k_B T \log 2$. Moreover, W_{\max}^{CMD} diverges in the limits $P_0 \rightarrow 0, 1$, showing that the CMD can extract arbitrarily large amounts of work. Should this violate the second-law inequality (equation (2))? The answer is negative because when W_{\max}^{CMD} diverges, so does the information content of the stored sequences $0_n, 1_n$, preserving the general Landauer inequality $W \leq k_B T I$. In fact, work extraction cycles in the CMD require storing multiple-bit sequences of the class $0_n, 1_n$ (Fig. 1b), whose length diverges in the limits $P_0 \rightarrow 0, 1$ when the molecule changes compartment after many measurements. This is in contrast with the classical MD where work

¹Condensed Matter Physics Department, University of Barcelona, Barcelona, Spain. ²Laboratoire de Biochimie, Institute of Chemistry, Biology and Innovation (CBI), UMR 8231, ESPCI Paris/CNRS, PSL Research University, Paris, France. ³CIBER-BBN de Bioingeniería, Biomateriales y Nanomedicina, Instituto de Sanidad Carlos III, Madrid, Spain. *e-mail: fritort@gmail.com

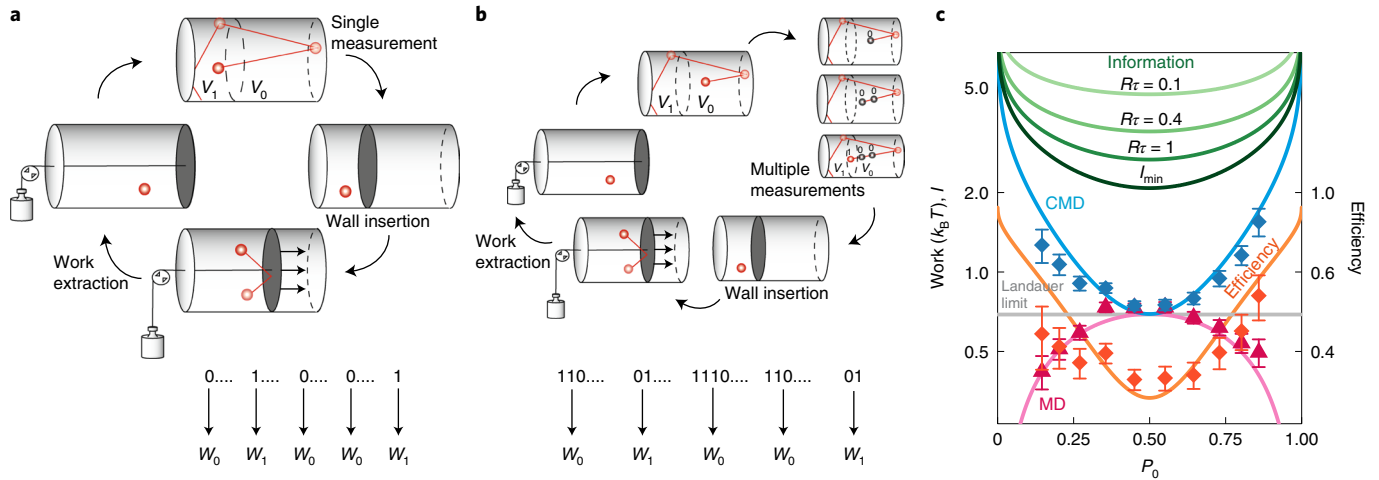


Fig. 1 | Classical MD versus CMD. **a**, In the classical MD, a single observation is made, and depending on the measurement outcome (0, 1), a work extraction process is implemented, which yields W_0 and W_1 values, respectively. **b**, In the CMD, multiple observations are made every τ , and a work extraction process is implemented when the molecule changes compartment (1 \rightarrow 0, 0 \rightarrow 1), yielding W_0 and W_1 values, respectively. The black dots indicated by 0 (upper right) indicate multiple measurements in the right vessel V_0 until the molecule changes compartment (0 \rightarrow 1). **c**, Work, information content and efficiency as a function of P_0 for the classical MD and the CMD. Mean work (classical MD: pink triangles; CMD: blue diamonds) obtained from the experiments (see Figs. 2 and 3) and theoretical prediction from equations (1) and (3) (pink and blue lines). The horizontal line shows $W_L = k_B T \log 2$. Information content in the CMD for different values of $R\tau$ (equations (4), (5) and (6)) from $R\tau = 0.1$ to $R\tau = \infty$ (light to dark green lines). Maximum efficiency in the CMD (equation (7)) obtained from experiments and theory (orange diamonds and line, scale on the right axis). In all cases, error bars represent the standard error of the mean.

extraction cycles require only a single-bit measurement (Fig. 1a). For a two-state system, with relaxation rate R , the average information content in the stored multiple-bit sequences can be exactly computed (Supplementary Section 1). It is given by $I(\tau) = I_{\min} + I_1(\tau)$, where $I_{\min} > 0$ is the minimum information content and $I_1(\tau) > 0$ is a monotonically decreasing function of τ such that $I_1(\tau \rightarrow \infty) = 0$. The expressions for I_{\min} and $I_1(\tau)$ are given by

$$I_{\min} = -\frac{P_0}{P_1} \log P_0 - \frac{P_1}{P_0} \log P_1 - P_0 \log P_1 - P_1 \log P_0 \quad (4)$$

$$I_1(\tau) = -\frac{P_0(P_0 + P_1 e^{-R\tau})}{P_1(1 - e^{-R\tau})} \log \left(1 + \frac{P_1}{P_0} e^{-R\tau} \right) - \frac{P_1(P_1 + P_0 e^{-R\tau})}{P_0(1 - e^{-R\tau})} \log \left(1 + \frac{P_0}{P_1} e^{-R\tau} \right) - \left(\frac{P_0 \log(P_0)}{P_1} + \frac{P_1 \log(P_1)}{P_0} \right) \frac{e^{-R\tau}}{1 - e^{-R\tau}} \quad (5)$$

The minimum information content is obtained in the limit $R\tau \gg 1$, where $I_1(\tau) = -e^{-R\tau} (P_0 \log(P_0)/P_1 + P_1 \log(P_1)/P_0) + O(e^{-2R\tau})$, whereas a diverging value is obtained for $R\tau \ll 1$: $I_1(\tau \rightarrow 0) = -\log(R\tau) + 1 + \frac{P_0^2 \log(P_0)}{P_1} + \frac{P_1^2 \log(P_1)}{P_0}$, giving $I_{\max}(\tau) = -\log(R\tau) + 1 - \log P_0 - \log P_1$. The chain of inequalities follows:

$$W \leq W_{\max}^{\text{CMD}} < k_B T I_{\min} < k_B T I(\tau) < k_B T I_{\max}(\tau) \quad (6)$$

We stress that W_{\max}^{CMD} is independent of τ . The lowest value of I_{\min} in equations (4) and (6) is obtained for $P_0 = P_1 = 1/2$, $I_{\min} = 3 \log(2)$, with stored sequences containing three bits on average. This is in contrast with the classical MD where the information content of one-bit sequences is equal to $\log(2)$. In fact, the CMD must store at

least two bits per cycle (the first bit defining the cycle class, the last bit closing the cycle when the molecule changes compartment). The efficiency of the CMD is defined by the ratio of W_{\max}^{CMD} (equation (3)) to the energy required to erase the stored sequences, $Q = k_B T I$. Maximum efficiency ϵ_{\max} is obtained in the limit $\tau \rightarrow \infty$:

$$\epsilon_{\max} = \frac{W_{\max}^{\text{CMD}}}{k_B T I_{\min}} = \left(1 + \frac{P_0 \log(P_0)/P_1 + P_1 \log(P_1)/P_0}{P_0 \log(P_1) + P_1 \log(P_0)} \right)^{-1} < 1 \quad (7)$$

Interestingly, for $P_0 = P_1 = 1/2$, the efficiency is minimal in the CMD ($\epsilon_{\max} = 1/2$), whereas it is maximal in the classical MD ($\epsilon_{\max} = 1$). Instead, in the limits $P_0 \rightarrow 0, 1$ the CMD yields $\epsilon_{\max} \rightarrow 1$. The behaviour of W_{\max}^{MD} , W_{\max}^{CMD} , $I(\tau)$, I_{\min} , ϵ_{\max} is shown in Fig. 1c (continuous lines). Note that for uncompressed sequences (that is, containing redundant information), the efficiency is lower than equation (7) (Supplementary Section 2).

Equation (5) shows that information content diverges in the continuum time limit $\tau \rightarrow 0$ when sequences contain an arbitrary large number of bits. However, it does so logarithmically, $I_{\max}(\tau) \rightarrow -\log(R\tau)$, rather than linearly with the number of bits, $I_{\max}(\tau) \rightarrow 1/R\tau$, showing that stored sequences are highly redundant for $\tau \ll 1/R$. A similar problem is found in data compression where information can be encoded using fewer bits than in the original representation¹⁷. In general, the information content of sequences, storing the outcome of measurements repeated at τ , diverges logarithmically for τ smaller than the de-correlation time.

Recent technological advancements have made possible the practical implementation of Szilard engines^{9,10,13}. Here, we report a room-temperature nanoscale Szilard engine composed of a single DNA molecule manipulated by optical tweezers (Fig. 2a). In our experiments, a single DNA hairpin was tethered between two micrometre-sized plastic beads (Materials and methods). The force applied on the molecule was controlled and measured, varying the position of the optical trap, λ . Under a suitable force, the molecule will exhibit spontaneous fluctuations between the folded and the unfolded states. This is equivalent to the initial state of the Szilard engine, where the

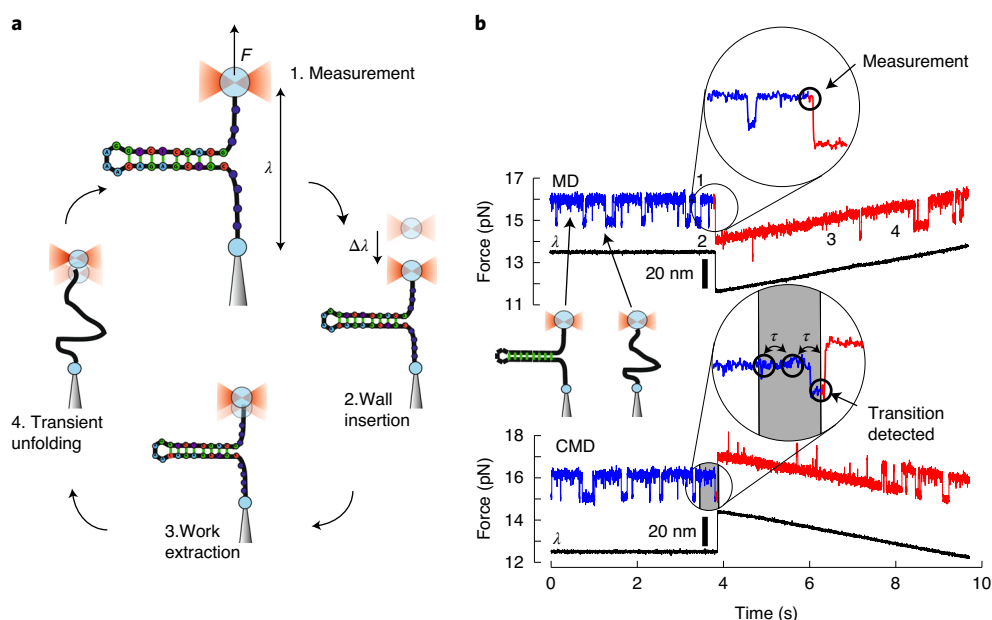


Fig. 2 | Single-molecule tests for the classical MD and CMD. **a**, Schematics of the steps in a work extraction cycle in a DNA hairpin pulling experiment. If the DNA hairpin is found in the folded state (step 1), the trap is suddenly approached by a distance $\Delta\lambda$ and the force F is relaxed (step 2). A work extraction process is implemented in which the trap slowly recovers the original position λ (steps 3 and 4). Work is extracted every time the molecule spontaneously unfolds. An equivalent cycle is implemented if the molecule is found in the unfolded state. **b**, Implementation of the work extraction process in the classical MD (upper traces) and the CMD (lower traces). Typical force-time traces before the work extraction process (hopping trace, blue) and during the work extraction adiabatic process (tilted hopping trace, red). The characteristic trap-position versus time stepwise function is shown in black.

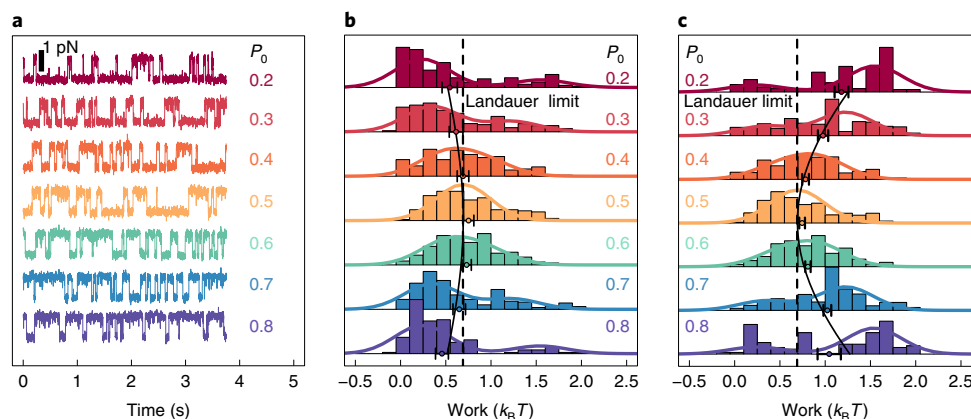


Fig. 3 | Extracted work distributions. **a**, Hopping traces at different values of P_0 . **b, c**, Extracted work histograms in the classical MD (**b**) and in the CMD (**c**) at the corresponding values of P_0 . Histograms are fit to double-Gaussian distributions (continuous coloured lines). The black circles are the mean of the extracted work distributions, and the solid black lines are the theoretical prediction, equation (1) for the classical MD (**b**) and equation (3) for the CMD (**c**). The vertical dashed lines are the Landauer limit. Error bars represent the standard error of the mean.

molecule can freely transition from the left to the right compartment. In the classical MD, the state of the DNA hairpin is observed at a given time, and depending on whether it is folded or unfolded, a pulling protocol to extract work is implemented, using the DNA as a pulley device (Fig. 2b, top). In the CMD, the state of the hairpin is monitored every τ , and the same protocol is implemented when the molecule changes state (Fig. 2b, bottom). The work extraction protocol is cyclic, that is, the control parameter λ is first driven away from its initial value λ_0 and then driven back to it. Whereas the first, forward, part of the protocol is swift (irreversible), the second, reverse part, is slow (adiabatic). Less work is consumed in the forward part of the protocol than can be extracted in the reverse part, yielding

a net amount of extracted work (Supplementary Section 3). It is possible to show that dissipation losses during the work extraction cycle are negligible (Supplementary Section 4). The spontaneous hopping events observed in the adiabatic part of the protocol (Fig. 2b, red traces) are the equivalent of the collisions against the inserted wall in the one-molecule Szilard gas and contribute to net work extraction. Let the bit 0 (1) denote the folded (unfolded) state. We have $P_0 = \frac{1}{1 + e^\phi}$ and $P_1 = \frac{1}{1 + e^{-\phi}}$, with ϕ being the equilibrium free-energy difference (in units of $k_B T$) between the folded and the unfolded states at λ_0 : $\phi = (G_0 - G_1)/k_B T = \Delta G/k_B T = -\log\left(\frac{P_0}{P_1}\right)$, where G is the Gibbs free energy.

A comparison of the results obtained for the classical MD and the CMD is shown in Fig. 3. In Fig. 3a, we show hopping traces at different equilibrium conditions ($-1.4 < \phi < 1.4$). Figure 3b,c shows the extracted work distributions together with the mean extracted work W_{\max} (circles) measured over many cycles in the classical MD and the CMD (work distributions being independent of the value of τ). The difference between both the work distributions and the mean extracted work is clear. Distributions are bimodal for $\phi \neq 0$, with larger amounts of work extracted from the CMD than from the classical MD. In particular, the Landauer limit (vertical dashed line) is an upper bound for the classical MD, but a lower bound for the CMD. The Landauer limit is met in both cases at the coexistence point $P_0 = P_1 = 1/2, \phi = 0$. The measured values for W_{\max}^{MD} , W_{\max}^{CMD} and ϵ_{\max} are shown in Fig. 1c and compared with the theoretical predictions in equations (1), (3) and (7).

It is remarkable that the Landauer limit turns into a lower bound of the mean extracted work for the CMD (rather than an upper bound). The large amount of work that can be extracted in the CMD in the limit $|\phi| \gg 1$ comes at the price of the long time required to observe the system leaving the most probable state. In fact, the average cycle time in the CMD, t_c^{CMD} , is given by (Supplementary Section 1)

$$t_c^{\text{CMD}}/\tau = \frac{1}{1 - e^{-R\tau}} \left(\frac{1 + e^{2\phi}}{e^{\phi}} \right) + 1 > 3 \quad (8)$$

From equations (1) and (3), we obtain for the relative power between the two cases, $P_{\text{CMD}}/P_{\text{MD}} \rightarrow 1 - O(1/|\phi|)$ in the limit $|\phi| \gg 1$, showing that the extracted power of both engines is asymptotically the same. The advantage of the CMD with respect to the classical case is the large amount of work per cycle that can be extracted in the CMD (Fig. 3c). This originates from the potentially unlimited information content of the stored sequences, which in the one-bit classical MD cannot exceed $\log(2)$. Moreover, the CMD captures rare dynamic events that deliver large amounts of work, whereas the classical MD captures typical events that yield only a moderate amount (Supplementary Section 5). The fact that the average power is asymptotically the same does not imply that the power distributions for finite time are equal. In fact, the work distributions obtained for the classical MD and the CMD (Fig. 3b,c) are already different, meaning that the distributions of power for finite time will be different too. The analytical calculation of such power distributions requires the application of large deviation theory, as has been done in the case of fluctuating efficiencies in heat engines¹⁸.

Our calculation of the information content, based on the Shannon entropy of the stored sequences, follows the spirit of the path thermodynamics approach applied to other non-equilibrium systems¹⁹. Although other information theoretical quantities introduced in the field of dynamic systems might be suitable to analyse our experimental data^{20,21}, all probably give the same result in the rare events limit $|\phi| \gg 1$. Furthermore, our information-content calculation might be extended to other non-equilibrium situations where work extraction is fuelled by rare dynamic events, such as in the context of fluctuation theorems for repeated feedback²² or machines with temporal correlations^{23,24}.

Finally, the CMD might be applicable to other contexts such as biological and quantum systems^{25,26}. For example, the CMD might be relevant in regulatory biological networks when the concentration of molecular species reaches a given threshold, such as during the generation and transmission of action potential signals across the cell membrane and signal transduction processes in general²⁷. In all these cases, there is a continuously monitored physical variable, and the cell responds when such a variable changes abruptly. For example, the action potential signal is generated when the potential difference across the cell membrane reaches a threshold. In this case, the work extracted would be equal to the free energy required to produce

that action potential signal at a specific membrane location, whereas information would be contained in the stored trains of bits defined by an inactive (0) or active (1) membrane potential relative to the threshold. We cannot avoid wondering whether the information-to-energy conversion in the CMD might have consequences in self-organization and selection processes taking place during the evolution of biological matter²⁸. The astonishing complexity of living matter might be seen as the outcome, over long evolutionary timescales, of a large work extraction process (used to build new and emergent high-free-energy structures) in environments suitable to store large amounts of information utterly erased by noise and randomness.

Online content

Any methods, additional references, Nature Research reporting summaries, source data, statements of data availability and associated accession codes are available at <https://doi.org/10.1038/s41567-019-0481-0>.

Received: 16 January 2019; Accepted: 22 February 2019;

Published online: 01 April 2019

References

- Leff, H. S. & Rex, A. F. (eds) *Maxwell's Demon: Entropy, Information, Computing* (Adam Hilger, 1990).
- Landauer, R. Irreversibility and heat generation in the computing process. *IBM J. Res. Develop.* **5**, 183–191 (1961).
- Bennett, C. H. The thermodynamics of computation: a review. *Int. J. Theor. Phys.* **21**, 905–940 (1983).
- Sagawa, T. & Ueda, M. Generalized Jarzynski equality under nonequilibrium feedback control. *Phys. Rev. Lett.* **104**, 090602 (2010).
- Sagawa, T. Thermodynamic and logical reversibilities revisited. *J. Stat. Mech.* **2014**, P03025 (2014).
- Parrondo, J. M. R., Horowitz, J. M. & Sagawa, T. Thermodynamics of information. *Nat. Phys.* **11**, 131–139 (2015).
- Seifert, U. Stochastic thermodynamics, fluctuation theorems, and molecular machines. *Rep. Prog. Phys.* **75**, 126001 (2012).
- Ciliberto, S. Experiments in stochastic thermodynamics: short history and perspectives. *Phys. Rev. X* **7**, 021051 (2017).
- Toyabe, S., Sagawa, T., Ueda, M., Muneyuki, E. & Sano, M. Experimental demonstration of information-to-energy conversion and validation of the generalized Jarzynski equality. *Nat. Phys.* **6**, 988–992 (2010).
- Berut, A. et al. Experimental verification of Landauer's principle linking information and thermodynamics. *Nature* **483**, 187–190 (2012).
- Mandal, D. & Jarzynski, C. Work and information processing in a solvable model of Maxwell's demon. *Proc. Natl Acad. Sci. USA* **109**, 11641–11645 (2012).
- Jun, Y., Gavrilov, M. & Bechhoefer, J. High-precision test of Landauer's principle in a feedback trap. *Phys. Rev. Lett.* **113**, 190601 (2014).
- Koski, J. V., Maisi, V. F., Pekola, J. P. & Averin, D. V. Experimental realization of a Szilard engine with a single electron. *Proc. Natl Acad. Sci. USA* **111**, 13786–13789 (2014).
- Roldan, E., Martínez, I. A., Parrondo, J. M. R. & Petrov, D. Universal features in the energetics of symmetry breaking. *Nat. Phys.* **10**, 457–461 (2014).
- Hong, J., Lambson, B., Dhuey, S. & Bokor, J. Experimental test of Landauer's principle in single-bit operations on nanomagnetic memory bits. *Sci. Adv.* **2**, e1501492 (2016).
- Peterson, J. P. S. et al. Experimental demonstration of information to energy conversion in a quantum system at the Landauer limit. *Proc. R. Soc. A* **472**, 20150813 (2016).
- Cover, T. M. & Thomas, J. A. *Elements of Information Theory* (Wiley, 1991).
- Verley, G., Esposito, M., Willaert, T. & Van den Broeck, C. The unlikely Carnot efficiency. *Nat. Commun.* **5**, 4721 (2014).
- Garrahan, J. P. Aspects of non-equilibrium in classical and quantum systems: slow relaxation and glasses, large deviations, quantum non-ergodicity, and open quantum dynamics. *Physica A* **504**, 130–154 (2018).
- Schreiber, T. Measuring information transfer. *Phys. Rev. Lett.* **85**, 461–464 (2000).
- Horowitz, J. M. & Sandberg, H. Second-law-like inequalities with information and their interpretations. *New J. Phys.* **16**, 125007 (2014).
- Horowitz, J. M. & Vaikuntanathan, S. Nonequilibrium detailed fluctuation theorem for repeated discrete feedback. *Phys. Rev. E* **82**, 061120 (2010).
- Schmitt, R. K., Parrondo, J. M. R., Linke, H. & Johansson, J. Molecular motor efficiency is maximized in the presence of both power-stroke and rectification through feedback. *New J. Phys.* **17**, 065011 (2015).
- Admon, T., Rahav, S. & Roichman, Y. Experimental realization of an information machine with tunable temporal correlations. *Phys. Rev. Lett.* **121**, 180601 (2018).

25. Pekola, J. P. Towards quantum thermodynamics in electronic circuits. *Nat. Phys.* **11**, 118–123 (2015).
26. Esposito, M., Harbola, U. & Mukamel, S. Nonequilibrium fluctuations, fluctuation theorems, and counting statistics in quantum systems. *Rev. Mod. Phys.* **81**, 1665–1702 (2009).
27. Ito, S. & Sagawa, T. Maxwell's demon in biochemical signal transduction with feedback loop. *Nat. Commun.* **6**, 7498 (2015).
28. Bialek, W. *Biophysics: Searching for Principles* (Princeton Univ. Press, 2012).

Acknowledgements

We acknowledge financial support from grants 308850 INFERNOS, 267862 MAGREPS (FP7 EU programme) FIS2013-47796-P, FIS2016-80458-P (Spanish Research Council) and ICREA Academia prize 2013 (Catalan government). M.R.-C. has received funding from the EU Horizon 2020 research and innovation programme under the Marie Skłodowska-Curie grant agreement no. 749944.

Author contributions

M.R.-C. performed the experiments. F.R. performed the theoretical calculations. Both authors planned the research and contributed to data analysis and preparation of the manuscript.

Additional information

Supplementary information is available for this paper at <https://doi.org/10.1038/s41567-019-0481-0>.

Reprints and permissions information is available at www.nature.com/reprints.

Correspondence and requests for materials should be addressed to F.R.

Publisher's note: Springer Nature remains neutral with regard to jurisdictional claims in published maps and institutional affiliations.

© The Author(s), under exclusive licence to Springer Nature Limited 2019

Methods

Experiments were performed with a highly stable miniaturized optical tweezers set-up²⁹. Two tightly focused counterpropagating laser beams (power 200 mW, wavelength 845 nm) were used to create a single optical trap. Experiments were carried out in a microfluidics chamber. Force measurements, based on detection of light momentum changes, were performed using position-sensitive detectors to measure the deflection of the laser beam after it interacted with the trapped object. The position of the trapping beam defines λ , which was measured by diverting ~8% of each laser beam to a secondary position-sensitive detector. The instrument resolution was 0.1 pN and 1 nm at a 1 kHz acquisition rate. In the experiments, a molecular construct consisting of a 20 bp DNA hairpin flanked by two short 29 bp DNA handles (labelled with biotin and digoxigenin) was tethered between two polystyrene beads. One type of bead was optically trapped, whereas the other bead was immobilized on the tip of a micropipette by air suction. Each handle could selectively bind to either streptavidin- (1.87 μ m, SpheroTech) or antidigoxigenin-coated beads (3.0–3.4 μ m,

Kisker Biotech). The synthesis protocols for short (20 bp) DNA hairpins have been previously described³⁰. All experiments were performed at 25 °C in a buffer containing 10 mM Tris, 1 mM EDTA, 100 mM NaCl and 0.01% NaN₃ (pH 7.5).

Data availability

The data that support the plots within this paper and other findings of this study are available from the authors upon reasonable request.

References

29. Huguet, J. M. et al. Single-molecule derivation of salt dependent base-pair free energies in DNA. *Proc. Natl Acad. Sci. USA* **107**, 15431–15436 (2010).
30. Camunas-Soler, J., Alemany, A. & Ritort, F. Experimental measurement of binding energy, selectivity, and allostery using fluctuation theorems. *Science* **355**, 412–415 (2017).